4782 *Macromolecules* **2010**, *43*, 4782–4790
DOI: 10.1021/ma100357h

Macromolecules
ARTICLE

Volume Transition of PNIPAM in a Nonionic Surfactant Hexagonal Mesophase

V. J. Jijo, Kamendra P. Sharma, R. Mathew,† Samruddhi Kamble, P. R. Rajamohanan,† T. G. Ajithkumar,† M. V. Badiger, and Guruswamy Kumaraswamy*

Complex Fluids and Polymer Engineering, National Chemical Laboratory (NCL), Pune 411008, India. † *Central NMR Facility, NCL, Pune, India*

Received February 16, 2010; Revised Manuscript Received April 12, 2010

ABSTRACT: We investigate the volume transition of a thermoresponsive polymer, poly(*N*-isopropylacrylamide), PNIPAM, in the presence of an aqueous solution of nonionic surfactant, $C_{12}E_9$. We combine turbidimetry with optical microscopy, NMR, and SAXS to follow the volume transition of the PNIPAM and the H_1-isotropic transition of the surfactant/water system. Nonionic surfactants such as $C_{12}E_9$ are known to interact weakly with PNIPAM. Accordingly, we show that there is only a small change in the volume transition temperature for the PNIPAM in isotropic micellar solutions of $C_{12}E_9$, even for relatively high concentrations of $C_{12}E_9$. Interestingly, once the surfactant forms an H_1 phase, there is a dramatic decrease in the coil−globule transition onset temperature. We believe that this behavior results from a competition between $C_{12}E_9$ in the H_1 phase, and PNIPAM to associate with water. When PNIPAM in the H_1 phase is cooled to low enough temperatures so as to be in the coil state, it locally disturbs the hexagonal phase ordering. Thus, we show that for PNIPAM in a weakly interacting surfactant matrix, it is the phase behavior of the matrix rather than the matrix chemistry that governs the coil−globule transition. Finally, we show that in a PNIPAM copolymer with a higher LCST we observe an interesting sequence of transitions in the surfactant phase: on cooling from a high temperature free-flowing turbid globular state (∼75 °C), we enter a free-flowing translucent coil phase (∼47 °C), then a turbid gel (∼25 °C) where the copolymer is collapsed in the H_1 phase, and finally a low-temperature clear gel (∼5 °C) where the copolymer is in the expanded coil state.

Introduction

On heating an aqueous solution of poly(*N*-isopropylacrylamide) (PNIPAM) to above its lower critical solution temperature (LCST) of around 32 °C, the polymer chains collapse and aggregate, and the solution goes from clear to cloudy. This transition of a PNIPAM chain from solvated coil to collapsed globule is entropically driven—Shibayama et al.[1] have estimated that, during the collapse transition, 13 molecules of water are liberated per monomer unit. The gain in translational entropy by liberating these water molecules drives the collapse of the polymer chain. The coil−globule transition of PNIPAM is reversible, and PNIPAM chains are rehydrated on cooling to below the LCST. The reversible, thermoresponsive nature of PNIPAM has prompted researchers to explore its use in applications ranging from controlled transport of ions through PNIPAM-grafted nanopores[2] to controlled delivery of drugs and biomolecules.[3,4]

The LCST of PNIPAM can be tailored by controlling the incorporation of hydrophobic or charged comonomers to decrease or increase the LCST, respectively.[5−7] The LCST is also strongly influenced by the addition of salts—typically, there is a decrease in the LCST with addition of salt.[8] Recently, Freitag et al.[9] showed that for a series of potassium salts (with the exception of potassium iodide) the decrease in LCST correlated with the position of the anions in the Hofmeister series. They suggest that the "salt effect" relates to the ability of the salt to influence the structure of water. Kim et al.[10] have demonstrated a decrease in polymer LCST on addition of saccharides and suggest that this decrease may be attributed to the change in the structure of water on solubilization of saccharides. Recent NMR studies indicate that the decrease in PNIPAM LCST by codissolution with small aromatic molecules cannot be rationalized by the effect of the additive on solvent structure alone, and specific additive-PNIPAM interactions also play a role in the decrease in LCST.[11] Addition of surfactants to PNIPAM has also been shown to dramatically alter the LCST. As early as 1978, it was shown that an aqueous solution of PNIPAM containing about 35 mM of an anionic surfactant, sodium dodecyl sulfate (SDS), does not exhibit precipitation even on heating to boiling.[9]

The majority of the studies on surfactant−PNIPAM interactions focus on anionic surfactants, specifically SDS. Meewes et al.[12] demonstrated that SDS increases the LCST of PNIPAM and that it can solubilize the polymer above its normal LCST by preventing aggregation and precipitation of the polymer. Schild and Tirrell[13] investigated the influence of *n*-alkyl sulfates of systematically varying chain lengths on the LCST of PNIPAM. They demonstrated that surfactants with an alkyl chain length of less than 4 carbon atoms decreased the LCST of PNIPAM and did not exhibit enhanced aggregation in the presence of polymer. However, for larger chain surfactants, both surfactant aggregation and the polymer LCST are affected by codissolution. For example, the authors claim that, in the presence of PNIPAM, SDS forms aggregates at concentrations that are an order of magnitude below its critical micellar concentration. At the same time, the LCST of the PNIPAM is also increased significantly due to the binding of surfactant micelles on the polymer chain. Ricka et al.[14] claim that the addition of small amounts of SDS leads to

*Corresponding author: Tel +91-20-2590-2182; Fax +91-20-2590-2618; e-mail g.kumaraswamy@ncl.res.in.

 Published on Web 04/20/2010

stabilization of PNIPAM globules (that they term "intermolecular" stabilization) while at higher concentrations (> 400 mg/L), where the SDS can aggregate, the PNIPAM chain expands due to association of SDS micelles along the polymer chain. Lee et al.[15] have used small-angle neutron scattering (SANS) to study the SDS−PNIPAM interactions and claim that, at high concentrations of SDS, surfactant micelles decorate the polymer chain to form a pearl-necklace structure. Wu et al.[16] have used conductometric titrations to study the collapse transition of PNIPAM in the presence of SDS and find that there are two transitions—the first of which they assign to SDS−PNIPAM binding and a second transition, the origin of which is not yet clear. The addition of SDS also influences PNIPAM chain−chain interactions, and reports[17] suggest that the viscosity of PNIPAM is higher in the presence of SDS below the LCST. While anionic surfactants typically increase the LCST of PNIPAM, a recent study claims that a biocompatible anionic surfactant, sodium cholate, slightly decreases the LCST of PNIPAM due to salt-induced aggregation of the polymers.[18]

Recent calorimetric studies indicate that the interaction of PNIPAM with anionic surfactants is favored over cationic surfactants.[19] For cationic surfactants, the size of the alkyl tail and that of the headgroup are believed to influence the interactions with PNIPAM. For hydrophobically modified fluorescently tagged PNIPAM, studies[20] show that both cationic and anionic surfactants bind to the polymer via hydrophobic interactions to form micelles along the chain that incorporate the hydrophobic moieties on the polymer and that both cationic and anionic surfactants result in an increase in LCST. A similar increase in the deswelling temperature has also been observed for cross-linked PNIPAM gels.[21] The group of Wu[22] has reported that while SDS increases the LCST of monodisperse PNIPAM microgels significantly, a cationic surfactant with a similar tail group (dodecylpyridine bromide) does not show an equally pronounced effect. On the basis of this evidence, they conclude that it is not surfactant adsorption along the PNIPAM chain (and the resultant headgroup−headgroup repulsions) that drive swelling of the microgels and the increase in LCST—rather, they claim that these phenomena result from the osmotic stress of surfactant micelles. They report that the cationic surfactant decreases the PNIPAM LCST at concentrations below the critical micelle concentration and increases the LCST at higher concentrations when the surfactant micelles swell the microgel. It is also worth mentioning recent studies[23] that demonstrate that layer-by-layer assembly of polyelectrolytes on PNIPAM microgel particles can influence microgel swelling temperature and swelling characteristics.

Previous studies indicate that nonionic surfactants do not significantly change the LCST of PNIPAM.[20,21] In codissolved PNIPAM/$C_{10}E_8$ surfactant systems ($C_{10}E_8$ is a nonionic surfactant with a C_{10} alkyl hydrophobic tail and eight ethylene oxide groups), studies reveal that adsorption at the air−water interface is competitive and is controlled only by the relative surface pressure of the surfactant and the polymer.[24] In contrast, in PNIPAM/SDS systems, the adsorption behavior is more complex and is governed by the association between the polymer and surfactant.[24,25]

FTIR suggests that the interaction of PNIPAM with a nonionic polymer, poly(ethylene glycol) (PEG), is very weak.[26] Calorimetric data show that the heat associated with the collapse transition is lower in the presence of PEG, and the authors claim that this is indicative of PEG competing with PNIPAM to complex water molecules.[26] The authors claim that the presence of PEG disturbs the hydration layer around PNIPAM, and the LCST is decreased as hydrophobic groups are exposed. For low molecular weight PEG (400 g mol^{-1}), there is a linear decrease in the LCST with increase in PEG concentration (LCST decreases by about 5 °C for 30% PEG solution). For entangled solutions of higher molecular weight PEG (10 000 g mol^{-1}), the decrease in LCST is nonlinear with polymer concentration; the specific heat peak broadens and becomes asymmetric, and there is hysteresis between heating and cooling runs. For high molecular weight PEG, the authors suggest that the PNIPAM chains are "trapped" in the network of PEG entanglements in solution and that the widening of the calorimetric transition and the hysteresis is indicative of the dispersity in the size of the PNIPAM aggregates in the soft PEG network.

Recently, researchers[27] have studied the incorporation of low concentrations (~0.17%) of hydrophobically modified PNIPAM copolymer in a monoolein cubic phase, with a view to controlling the release of small molecules encapsulated in the surfactant phase. However, the effect of the cubic phase on the copolymer volume transition was not reported.

In this work, we examine the volume transition of PNIPAM homo- and copolymers in the presence of a nonionic surfactant, $C_{12}E_9$, and contrast the behavior of PNIPAM in a micellar phase of the surfactant and in a hexagonal mesophase. Our group has previously investigated polycondensation of cross-linked silicones in surfactant mesophases[28,29] and has shown that polymer particles with rodlike and sheetlike morphologies can be formed due to mesophase-mediated elastic interactions between growing polymer particles. In more recent work, we have demonstrated[30] that when preformed silica nanoparticles are dispersed in the hexagonal phase, the particle−mesophase composite structure is particle size dependent. For small particles, (particle size, $a <$ characteristic length scale for the mesophase, d), the particles swell the mesophase and d increases with particle loading. For $a \approx d$, there is a partitioning of particles between a dispersed phase and an aggregate phase, and for $a > d$, the particles phase separate from the mesophase to form a network of particulate strands. In this work, we study PNIPAM chains as they undergo a volume transition from an expanded chain state (where $R_g > \approx d$) to a collapsed globule (where $R_g < d$) and examine their behavior in a hexagonal mesophase of nonionic surfactant. On the basis of the previous literature, we anticipate that the nonionic surfactants used in this study do not interact strongly with the PNIPAM. Indeed, our results indicate that there is very little change in the LCST in the micellar surfactant phase, even up to high concentrations of surfactant. However, when the surfactant organizes into a hexagonal phase, there is a dramatic decrease in the LCST. We believe that this is the first systematic study that demonstrates that, in systems where the chemistry of the "matrix" dictates a weak interaction with PNIPAM, the LCST is more strongly influenced by the matrix *phase*.

Experimental Section

Nonionic surfactant nonaethylene glycol dodecyl ether ($C_{12}E_9$) was obtained from Sigma-Aldrich and was used as received (HPLC previously reported[24]). Distilled deionized water (resistivity = 18.2 MΩ·cm) from a Millipore Milli-Q unit was used to prepare the surfactant mesophases. The PNIPAM homopolymer used was synthesized as described in previous literature.[31] Intrinsic viscosity measurements indicate that the PNIPAM has a molecular weight, $M_v = 10\,500$ g mol^{-1}. Further characterization of the homopolymer is presented in the Supporting Information (FTIR, proton NMR, and hydrodynamic radius, R_h, in Figure S-char-1). To obtain a thermoresponsive copolymer with a higher LCST, we copolymerized *N*-isopropylacrylamide with acrylamide (~20 wt % acrylamide in the feed; both monomers from Acros Chemicals, used after recrystallization and vacuum drying) via free radical polymerization using potassium peroxodisulfate (Sigma-Aldrich) as initiator. The synthesis was carried out using a modified version of a previously

described protocol.[32] Polymerization was carried out in distilled deionized water at 70 °C under a nitrogen purge. Unreacted monomers were removed by dialysis against distilled deionized water for 2 days, after which the dialyzed sample was freeze-dried. We determined that the LCST of the copolymer synthesized is around 50 °C—this accords well with the values reported[33] for a 20 wt % acrylamide copolymer. Detailed characterization of the copolymer (FTIR, proton NMR, and R_h) is presented in the Supporting Information (Figure S-char-2). Neither the homopolymer nor the copolymer was specifically end-capped during synthesis.

Composites with the surfactant hexagonal phase were prepared by addition of PNIPAM solutions to the $C_{12}E_9$/water mixture at 50 °C, above the isotropic−H_1 transition temperature, vortexing and subsequently cooling to room temperature. The water in the PNIPAM solutions during addition was accounted for to calculate the ratio of the surfactant to water in the final composite. We report the surfactant wt % in the sample relative to the amount of surfactant and water (viz., considering that surfactant + water add to 100%). The PNIPAM content (in wt %) is reported relative to the amount of surfactant, water, and polymer. This makes it easy to compare the samples with and without PNIPAM. Thus, a sample containing 47.5 mg of surfactant, 47.5 mg of water, and 5 mg of PNIPAM is designated as a sample with 50% surfactant and 5% PNIPAM to make it easy to compare with a surfactant/water sample containing equal fractions of surfactant and water (viz. 50 mg of surfactant, 50 mg of water, and 0 mg of PNIPAM).

Optical microscopy was performed using an Olympus-BX 50 equipped with a crossed polarizer setup. Samples were mounted on a CSS-450 cell from Linkam, which we used as a hot stage to control the sample temperature. The sample temperature in the CSS-450 is controlled to within 0.1 °C, and we are able to control the sample cooling rate from 0.1 to 5 °C/min. The temperature measured by the Linkam hot stage was calibrated using liquid crystal standards (5CB and 8CB). We placed wet rags near the sample to minimize change in the sample water composition due to evaporation. The isotropic−hexagonal transition temperature for the surfactant/water system is determined by the (dis)-appearance of characteristic mesophase textures during temperature scan experiments. This transition temperature is sensitive to the water concentration in our sample. We observe that there is no change in the measured transition temperature for two repeat temperature cycles (heat−cool−heat−cool), suggesting that there is no significant water evaporation during our experiments.

Turbidity measurements were performed using a setup built in our laboratory. Laser light (HeNe, $\lambda = 632.8$ nm, 5 mW, Melles Griot) transmitted through a sample mounted on a temperature-controlled CSS 450 Linkam cell was measured using a detector (PDA-55, Thor Laboratories). The detector signal was logged using a home-built LabView-based data acquisition system, using a standard A/D card (National Instruments). For the turbidity measurements, the sample was loaded on the bottom plate of the CSS-450. A coverslip was placed on the sample, and the sample was manually pressed to approximately the same thickness (around 20−25 μm). The sample was then heated to 50 °C and cooled at a controlled rate while the intensity of transmitted laser light was recorded. The sample was subsequently heated from a low temperature to 50 °C, and transmitted intensity was recorded for the heating run also. Measurements were repeated on at least two independent samples to ensure reproducibility. We also repeated a temperature cycle on the same sample to confirm that there is no significant water evaporation during our experiment.

NMR measurements were conducted on a Bruker AV400 NMR spectrometer operating at 400 and 100 MHz for ^{1}H and ^{13}C, respectively. A standard 5 mm broad band observe (BBO) gradient probe was used. Samples for NMR measurements were prepared by dissolving required amounts of polymer and surfactant in 99.8% D_2O using the aforementioned sample preparation protocol. (Note that samples were prepared in D_2O only for NMR measurements. All other measurements were made in samples prepared using distilled deionized water.) The samples were initially heated to 55 °C for 20 min in the NMR probe, and the spectra were acquired on cooling the samples to the required temperature. At each temperature the sample was allowed to equilibrate for 15 min. The ^{1}H and ^{13}C $\pi/2$ pulses were 14 and 12 μs, respectively. A Bruker BVT3200 unit was used for controlling temperature during the variable temperature measurements. For ^{13}C measurements, 2000 transients were collected using a 30° flip angle and 2 s relaxation delay, whereas 16 scans were employed for ^{1}H studies with a relaxation delay of 3 s. The ^{13}C spectra were acquired with NOE, i.e., by ^{1}H decoupling during acquisition and relaxation delay. The raw data were processed with 5 Hz line broadening prior to Fourier transformation. Peak areas were used for comparison of the data measured at different temperatures.

^{13}C spin−lattice relaxation time measurements were also done at 100 MHz. Spin−lattice relaxation times of the solutions were measured using a conventional $\pi-\tau-\pi/2-$Acq inversion recovery.[34,35] 64 transients were collected with a relaxation delay of 3.5 s with τ delays varying from 1 ms to 20 s in a pseudo-2D mode. The data were analyzed with the help of the Bruker T_1/T_2 analytical routine. NOESY and ROESY measurements were performed by using a standard 2D pulse sequences with a mixing time of 300 ms and spin lock (CW) time of 300 ms, respectively.[36]

Small-angle X-ray scattering (SAXS) measurments were performed using a Bruker Nanostar, equipped with a rotating anode generator, operating at 45 kV and 100 mA (copper anode, $\lambda = 1.54$ Å), three-pinhole collimation, and a 2-dimensional multiwire Histar detector. The SAXS detector was calibrated using silver behenate. Samples were mounted in quartz capillaries with a diameter of around 2 mm, and temperature control was via the Bruker hot stage. We calibrated the hot stage using the isotropic−nematic phase transition of 5CB. The capillary filled with gel sample after proper sealing was heated to 50 °C and held there for 5 min. The collimation tubes and flight path to the detector were evacuated, but the sample chamber was maintained at ambient pressure. Data were acquired and circularly averaged to convert to 1-dimensional format (intensity versus q) using the Bruker software.

Results and Discussion

Our results are organized as follows: we first describe visual observations and temperature-dependent turbidity measurements on the PNIPAM/surfactant/water systems. Subsequently, we describe our NMR investigations and correlate these with the turbidity measurements. We then characterize the structure of our systems using polarized optical microscopy and SAXS. Finally, we describe preliminary experiments with a PNIPAM copolymer in surfactant/water to validate the inferences from our studies on the PNIPAM/surfactant/water systems.

Visual Observations and Turbidity Measurements. At 50 °C, a 5% (by weight) aqueous solution of PNIPAM is turbid and has a low viscosity (Figure 1, vial 2, top). On cooling, the solution becomes clear at about 34 °C and stays clear at room temperature and at 5 °C (Figure 1, center). When we consider a 50% (by weight) nonionic surfactant, $C_{12}E_9$/water mixture, we observe that it is a clear, free-flowing solution at 50 °C and that, on cooling, it forms a clear gel at about 44 °C (Figure 1, left, vial 1). At room temperature and at 5 °C, the $C_{12}E_9$/water mixture exists as a transparent gel. Now, when we consider a system containing equal parts by weight of $C_{12}E_9$ and water, and 5 wt % PNIPAM, we observe that it is a free-flowing, turbid liquid at 50 °C, that transitions to a turbid gel at room temperature, and that becomes a transparent gel on further cooling to 5 °C (Figure 1, right, vial 3).

Here, the onset of gelation in systems containing $C_{12}E_9$ and water is associated with the transition from a

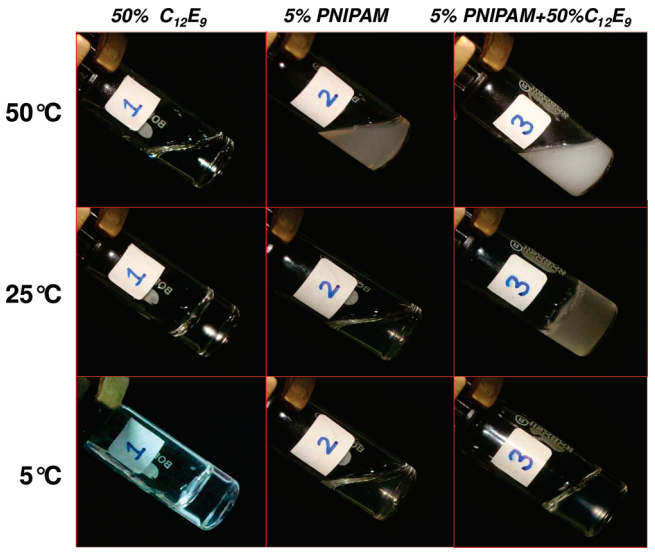

Figure 1. Photographs of 50% $C_{12}E_9$−50% water system (left column), 5% (by weight) PNIPAM in water (middle column), and 5% PNIPAM−50% $C_{12}E_9$ (right column) at different temperatures. The top row is at low temperature (5 °C), the middle row is at room temperature, and the bottom row is at 50 °C. The sample vials are tilted to distinguish the low-viscosity materials from the gels.

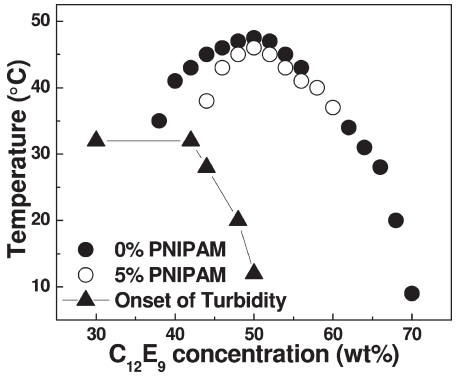

Figure 2. Phase diagram identifying the isotropic−H_1 transition temperature (circles) and the temperature at which there is an onset of turbidity (triangles). The surfactant concentration is specified as explained in the text, so that the samples with and without PNIPAM can be easily compared. The filled circles represent data for the surfactant/water system, viz. in the absence of PNIPAM, while the open circles are for 5% PNIPAM in the surfactant/water system. The onset of turbidity on heating corresponds to the onset of the coil−globule transition for the PNIPAM (see text).

high-temperature, low-viscosity micellar state to a hexagonal mesophase comprising of hexagonally stacked cylindrical surfactant assemblies, with a cylinder spacing of ca. 5.6 nm. The formation of the hexagonal phase can be characterized by the appearance of birefringent, fan-shaped domains in polarized optical microscopy (see, for example, Figure 7h) and by the appearance of characteristic peaks in small-angle X-ray scattering[30] (SAXS, peaks at q values in the ratio of 1:$\sqrt{3}$; see also Supporting Information, Figure S8). We use polarized optical microscopy with a hot stage to map out the hexagonal−isotropic transition temperatures as a function of the surfactant/water ratio. As mentioned in the Experimental Section, we report the surfactant percentage for all samples relative to the amount of surfactant and water in the sample, while the PNIPAM percentage is reported relative to the amount of PNIPAM, surfactant, and water. This is done to facilitate comparison between samples with and without PNIPAM.

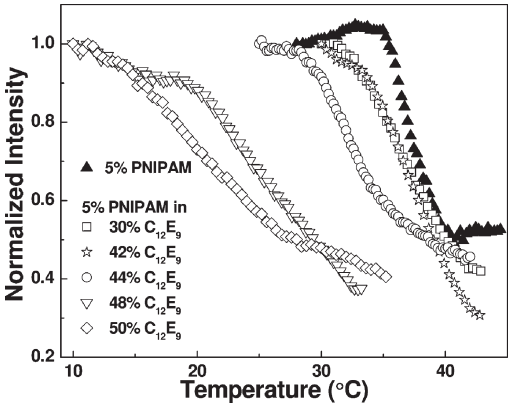

Figure 3. Intensity of light transmitted through the sample as a function of temperature on heating for 5% PNIPAM in water (filled symbols) and for 5% PNIPAM in various concentrations of surfactant (open symbols). The transmitted intensity [= $I(T)/I(5\ °C)$] is normalized by the low-temperature intensity.

We observe that addition of 5 w t% of PNIPAM to the $C_{12}E_9$/water system influences the H_1−isotropic phase transition (Figure 2). While in the neat $C_{12}E_9$/water system, the H_1 phase concentration window extends from a surfactant concentration of ∼36%, the addition of 5% PNIPAM suppresses formation of the H_1 phase until a surfactant concentration of about 43%. Further, there is a decrease in the isotropic−H_1 transition temperatures by a few degrees relative to the neat $C_{12}E_9$/water systems, on addition of PNIPAM (Figure 2). Systems containing PNIPAM exhibit turbidity on heating, which we show later, is associated with the polymer LCST. In Figure 3, we present results from turbidity measurements, after normalizing the intensity of light transmitted through the sample with the transmitted intensity at low temperatures (viz. when the sample is transparent). The data in Figure 3 represent experiments at a heating rate of 0.2 °C/min. Experiments at other heating rates (0.5 and 1 °C/min; Figure S1 in Supporting Information) gave qualitatively similar data. All heating experiments reported in Figure 3 were repeated at least two times at each surfactant concentration to ensure that the trends in the data were reproducible.

The temperature at which the onset of turbidity is observed on heating decreases only slightly on addition of surfactant up to concentrations of 42%, viz. when the surfactant is in the isotropic micellar state (∼32 °C vs ∼34 °C for surfactant-free PNIPAM solutions) (Figures 2 and 3). On heating a 5% solution of PNIPAM in water, the onset of turbidity (at ∼34 °C) is abrupt, and the sample becomes turbid rapidly as it is heated to about 40 °C (Figure 3). For solutions in the isotropic micellar state, containing 30% and 42% surfactant, the onset of turbidity is shifted to slightly lower temperatures, around 32 °C, and the sample increases in turbidity on heating to 40 °C (Figure 3), similar to the surfactant-free PNIPAM solution. For higher surfactant concentrations, viz. for samples in the H_1 phase, we see a dramatic decrease in the temperature for onset of turbidity—from 28 °C for 44% surfactant to 17 °C for 48% and 13 °C for 50% (Figures 2 and 3). Here, the development of turbidity is significantly more gradual, taking place over a temperature interval of about 15−20 °C for the 50% surfactant sample (Figure 3). For a surfactant concentration of up to 54%, we observed that samples containing PNIPAM turned clear only very near 0 °C (data not shown), and for surfactant concentrations > 54%, samples containing PNIPAM stayed turbid even when cooled to near the freezing temperature of water.

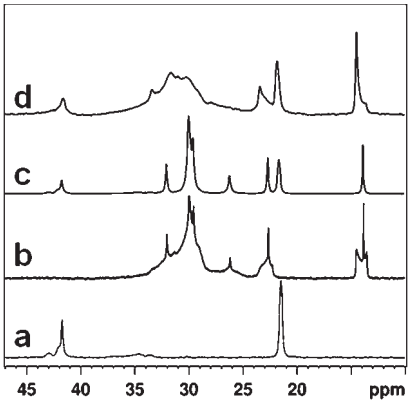

Figure 4. ^{13}C NMR spectra of the systems studied: (a) 5% aqueous PNIPAM, (b) surfactant H_1 phase (0% PNIPAM; 50% $C_{12}E_9$), (c) 5% PNIPAM−30% $C_{12}E_9$, and (d) 5% PNIPAM−50% $C_{12}E_9$. All spectra were acquired at room temperature (25 °C).

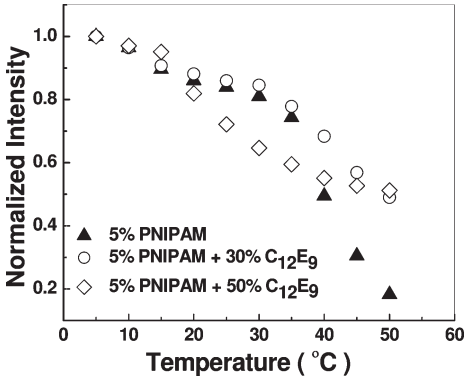

Figure 5. Temperature dependence of the area of methyl carbon signals of the polymer in 5% PNIPAM in D_2O, 5% PNIPAM−30% $C_{12}E_9$, and 5% PNIPAM−50% $C_{12}E_9$. The area of the signal at a particular temperature is normalized with the area of the same signal at 5 °C for each system.

There was no change in the turbidity of samples stored in sealed vials at room temperature over a period of several weeks, suggesting that the observed turbidity is not transient. Further, the development of turbidity during heating and during cooling scans is not significantly different, either for the PNIPAM aqueous solution or for the 50% surfactant system containing 5% PNIPAM (Figure S2, Supporting Information). Thus, our data suggest that the differences in the development of turbidity in the H_1 phase relative to the low-viscosity PNIPAM solutions are not due to kinetics or due to the enhanced viscosity of the hexagonal gel phase.

NMR Studies. In order to get more insight into the origin of the turbidity developed in our samples, we use NMR spectroscopic techniques to monitor the volume transition of PNIPAM. The PNIPAM LCST can be readily followed by various NMR spectroscopic techniques,[37] by monitoring either the water or the polymer as a function of temperature. For example, water molecules show considerable difference in their motional properties as PNIPAM undergoes collapse, and this is reflected in their relaxation time and in their self-diffusion coefficient.[38−43] Alternatively, NMR signals from PNIPAM show appreciable changes in their line width during the volume transition as a result of the expulsion of water.[44] As the proton signals from the polymer become too broad to be detected in the collapsed state in conventional ^1H NMR, the temperature dependence of the area under the PNIPAM proton peaks (either the backbone or the pendant isopropyl groups) can be used to monitor the volume transition.[45,46] We have verified that, for a surfactant-free 5% PNIPAM solution in D_2O, the polymer LCST can be followed by monitoring the area under the proton peaks in region from 0 to 1.8 ppm (data in Supporting Information, Figure S3). However, in the surfactant hexagonal phase, the isopropyl proton signal broadens, overlaps with the surfactant peaks, and is, therefore, not clearly visible (data in Supporting Information, Figure S4). Thus, we use ^{13}C NMR to follow the collapse transition of the PNIPAM since the peaks from the PNIPAM can be clearly differentiated from those from the surfactant (Figure 4). The aliphatic region of the ^{13}C NMR of PNIPAM shows two relatively sharp peaks corresponding to the carbons of the pendant isopropyl group (methyl group ∼21 ppm and the carbon bonded to the nitrogen near 42 ppm), which do not overlap with ^{13}C peaks from the surfactant (Figure 4). The backbone CH and CH_2 carbon signals are relatively broad and appear in the region $\delta = 41-43$ ppm and $\delta = 33-37$ ppm, respectively. From independent ^{13}C spin−lattice relaxation time measurements, we confirm that, for the conditions used (30° flip angle), the delay between scans (2 s) is adequate to ensure relaxation of the ^{13}C spins. No special care was taken to suppress $^1H-^{13}C$ hetero nuclear NOE's as we monitor only the relative change in peak area with temperature; hence, to a first approximation, changes in NOE factor, if any, can be neglected.

We have followed the methyl signal of PNIPAM (∼21 ppm) as a function of temperature for all the systems studied. For surfactant free 5% solutions of PNIPAM in D_2O, we have shown that the temperature-dependent decrease in the area of the PNIPAM ^{13}C methyl peak accords with the results from the ^1H experiments and tracks the volume transition (data in Supporting Information, Figure S5). Our results from heating experiments on 5% PNIPAM systems in 30% and 50% surfactant are summarized in Figure 5. In general, it is observed that the signal strength decreases gradually as the temperature is raised from 5 to 50 °C. In the initial stages (below the LCST), the signal decreases gradually with temperature—beyond a certain temperature, which we designate as the LCST, the decrease in the signal with increasing temperatures is more rapid. We now examine these data in more detail.

For the 5% aqueous solution of PNIPAM, we observe that the area under the PNIPAM peaks (of methyl carbons in the region from $\delta = 20.5$ to 22.5 ppm) decreases gradually on heating from 5 to 35 °C and decreases abruptly above 35 °C (Figure 5). The abrupt decrease at 35 °C corresponds to the volume transition or the LCST of the PNIPAM—the decrease in intensity correlates with a densification of the polymer coil and the consequent decrease in segmental mobility of the polymer segments on heating. The peak area at 50 °C is ∼10% of the initial peak intensity at 5 °C—in the literature, this has been attributed to PNIPAM units in a "dilute phase".[42]

For a 30% surfactant solution containing 5% PNIPAM, the initial gradual decrease in intensity is similar to that observed for the aqueous solution of PNIPAM (Figure 5). Above 30 °C, the decrease in peak intensity is distinctly more rapid—however, this decrease is not abrupt as for the aqueous PNIPAM solution at 35 °C. At 50 °C, the intensity of the PNIPAM peaks in the 5% PNIPAM−30% surfactant system decreases to about 50% of the signal at 5 °C—significantly higher than for the surfactant free 5% solution of PNIPAM (where the residual signal ∼10%).

For the 50% surfactant solution, the decrease in peak intensity starts at 15 °C and continues gradually until 50 °C

(Figure 5). Thus, the LCST of the PNIPAM from our NMR measurements (~35 °C for surfactant free PNIPAM, ~30 °C in 30% surfactant, and ~15 °C in 50% surfactant) correlate well with the values of turbidity onset (34 °C for surfactant free PNIPAM, 32 °C in 30% surfactant, and 13 °C in 50% surfactant; see Figure 3), especially when we consider the relatively coarse temperature resolution (5 °C) of our NMR experiments. This suggests that the turbidity measurements track the decrease in segmental mobility of the PNIPAM and are indicative of the LCST, even in the surfactant-containing systems. Interestingly, for PNIPAM in both 30% and 50% surfactant solutions, the final NMR intensities at 50 °C are roughly similar, at about 50% of the peak intensity at 5 °C. This indicates that 50% of the PNIPAM chain segments in surfactant solutions remain motionally averaged, even at 50 °C, compared to 10% in the surfactant-free case. Further, the NMR peak intensity (relative to that at 5 °C) for PNIPAM in 50% surfactant is lower compared to the surfactant free PNIPAM or PNIPAM in 30% surfactant between 20 and 35 °C. Thus, in the hexagonal phase, there are fewer mobile PNIPAM chains relative to the case of PNIPAM in surfactant-free conditions or in the presence of a micellar solution.

What is the origin of the residual NMR signal for the collapsed PNIPAM? We note that in the case of cross-linked PNIPAM systems (or for microgels) the extent of the residual signal is much lower than for linear PNIPAM chains.[47,48] Therefore, the residual signal for the surfactant-free PNIPAM in our experiments results from the single chain nature of our sample. In our experiments, when PNIPAM in a surfactant phase (either micellar 30% surfactant or hexagonal 50% surfactant) is heated, the residual signal increases to 50% of that at low temperature (compare with 10% residual signal for PNIPAM collapse in the absence of surfactant). It is possible that association of the surfactant with PNIPAM results in this behavior. To understand the surfactant−PNIPAM interactions, we resort to nuclear Overhauser enhancement (NOE) experiments.[49]

We employ 2D ROESY[34] for identification of protons that are spatially close for systems in the long correlation limit. In the conventional NOESY spectrum, cross-peaks between interacting protons are positive, and we observe strong cross-peaks among all the protons, even those that are relatively far apart, due to efficient spin diffusion (data in Supporting Information, Figure S6). In contrast, in the 2D ROESY spectrum, the spatial proximity is manifested as negative cross-peaks between the interacting proton signals, which are visible only for protons that are in close spatial proximity.[47] The ROESY spectrum for the 5% PNIPAM−30% surfactant system clearly shows the presence of negative cross-peaks between the methyl protons of the pendant isopropyl group of the PNIPAM and the OCH_2 groups of the surfactant (Figure 6; also see Supporting Information, Figure S7). Thus, our ROESY data provide unequivocal evidence for the interaction between PNIPAM and the nonionic surfactant.

Further, we also observe evidence for polymer−surfactant interactions in the ^{13}C NMR spectra (Figure 4). We note that the terminal methyl group of the surfactant in the 50% $C_{12}E_9$ mesophase (not containing PNIPAM) shows a characteristic anisotropic line shape (Figure 4b). On heating into the isotropic micellar phase, the line shape of this terminal methyl group gets converted to a Lorentzian (data not shown), as might be anticipated for the highly mobile, low-viscosity phase. Interestingly, for the 5% PNIPAM−50% surfactant sample, the line shape of the terminal methyl group of the surfactant at room temperature (Figure 4d) is very different from that of the surfactant mesophase not containing PNIPAM (Figure 4b). We believe that this difference in the line shape in the presence of PNIPAM is due to polymer−surfactant interactions. Thus, these observations of the influence of PNIPAM on the line shape, combined with the ROESY measurements, indicate that there are surfactant−PNIPAM interactions, unlike previous litearature reports,[20,21,26] and suggest that these interactions might be implicated in the higher residual signal of PNIPAM in the surfactant solution at 50 °C.

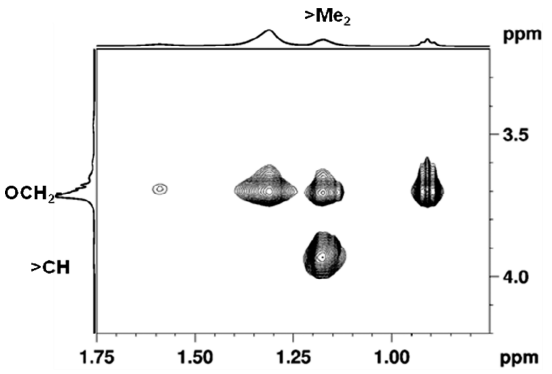

Figure 6. 400 MHz ROESY spectrum of PNIPAM in the micellar phase (30% $C_{12}E_9$). Only cross-peaks in the region of interest are shown. The polymer peaks corresponding to the pendant isopropyl groups are marked as >CH and $>Me_2$ while the proton signal of the surfactant is marked as $-OCH_2-$. Besides the cross-peak between $>Me_2$ of polymer and OCH_2 groups of the surfactant (intermolecular interaction), strong cross-peaks due to intraresidue interactions (between the $>Me_2$ and >CH of polymer and CH_2, CH_3, and OCH_2 of the surfactant) were also observed.

Structural Investigations. Optical microscopy of the PNIPAM/surfactant/water system provides us with information about the spatial organization of this system at length scales of several micrometers. For the 50% surfactant system containing 5% PNIPAM, we observe no structure under the microscope at 50 °C (Figure 7a,b). As the system is cooled to room temperature, we observe (between crossed polarizers, Figure 7d) the formation of fan-shaped domains characteristic of the hexagonal phase. Interestingly, in the corresponding image between parallel polarizers (Figure 7c), we observe dark structures at the boundaries of the hexagonal phase domains. These dark boundaries are not observed for the 50% surfactant hexagonal phase that does not contain PNIPAM (Figure 7g,h). Further, these boundaries disappear when the 50% surfactant−5% PNIPAM system is cooled to 5 °C (Figure 7e). Thus, this data suggests that the dark boundaries might comprise PNIPAM chains that are collapsed globules at room temperature in a 50% surfactant system and that phase separate from the hexagonal phase to accumulate at the H_1 phase domain boundaries. The aggregates of these collapsed chains scatter light and render the system turbid. On cooling to 5 °C, the PNIPAM chains rehydrate and thus are no longer visible under the optical microscope. Under these low-temperature conditions, the sample becomes visibly clear. From the optical micrographs (Figure 7), it is clear that the size of the fan-shaped hexagonal domains is larger for surfactant/water samples containing PNIPAM relative to the corresponding polymer-free samples. We do not know the precise reason for this. We observe that incorporation of the PNIPAM into surfactant/water suppresses the H_1−isotropic transition (Figure 2): it is possible that PNIPAM inhibits the nucleation of H_1 domains on cooling from the isotropic phase, thus resulting in the formation of larger hexagonal domains.

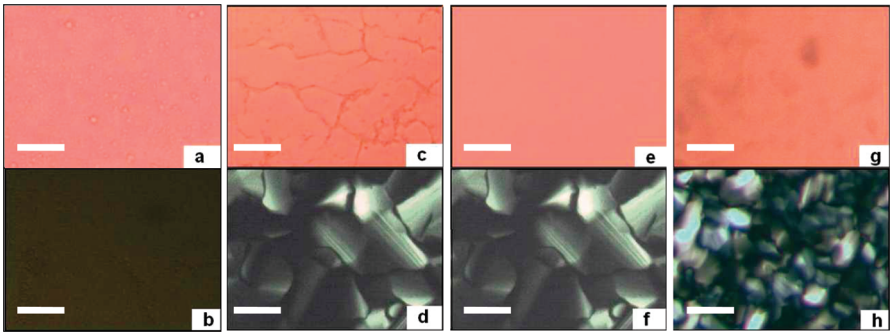

Figure 7. Optical micrographs observed between parallel polarizers (top row) and between crossed polarizers (bottom row) for (a, b) 5% PNIPAM−50% $C_{12}E_9$ at 50 °C (viz. in the low-viscosity, isotropic micellar state), (c, d) 5% PNIPAM−50% $C_{12}E_9$ at 25 °C (viz. in the turbid, high-viscosity H_1 gel phase), (e, f) 5% PNIPAM−50% $C_{12}E_9$ at 10 °C (viz. in the transparent, high-viscosity H_1 gel phase),and (g, h) 0% PNIPAM−50% $C_{12}E_9$ at 25 °C (viz. the surfactant H_1 gel not containing PNIPAM). The scale bar in all the images corresponds to 50 μm.

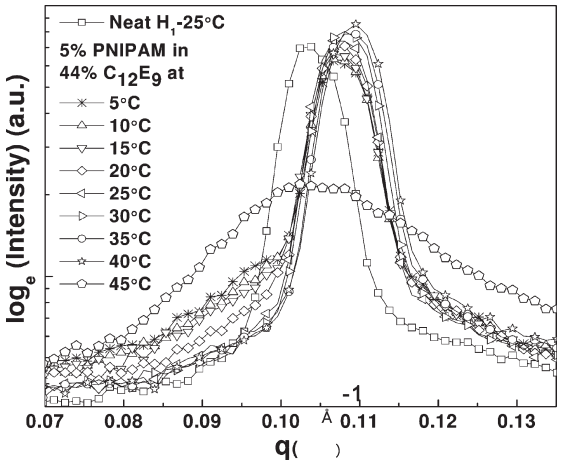

Figure 8. Small-angle X-ray scattering from the surfactant H_1 phase and from 5% PNIPAM−44% $C_{12}E_9$ on cooling from 45 to 5 °C. We present data in the q region where the primary peak from the H_1 phase and the isotropic micellar correlation peak are observed.

Further clues to the state of the micellar aggregates at different temperatures can be obtained from SAXS (Figure 8). At temperatures where the H_1 phase exists, we see peaks at about 0.105 A^{-1} and the corresponding secondary peaks at around 0.181 A^{-1} ($q_2 \approx \sqrt{3}q_1$, see Figure S8 in the Supporting Information). Thus, the presence of PNIPAM does not disturb H_1 phase formation. However, the systems containing PNIPAM show a hexagonal phase peak at larger q values relative to the neat surfactant/water hexagonal phase, suggesting that PNIPAM might act to competitively associate with water (Figure 8: note that, here, we present data on a sample containing 44% surfactant and 5% PNIPAM—however, qualitatively similar temperature-dependent behavior is observed at other surfactant concentrations). Thus, the surfactant concentration in the H_1 phase is higher than the nominal concentration in the system. On the basis of the H_1 peak positions of the surfactant/water system, we estimate that the surfactant concentration in the H_1 phase in the 44% sample, for which we present data is 46.7%. Similarly, for 48% and 50% surfactant samples containing 5% PNIPAM, the surfactant concentrations in the H_1 phase are 50% and 52.6%, respectively. On heating the hexagonal phase to above the isotropization temperature, we see the hexagonal phase peaks disappear and observe the broad hump that represents micellar correlations in the low-viscosity aqueous micellar state. Interestingly, we observe that on cooling to temperatures below the isotropic−H_1 phase transition broad "micelle-like" features appear that coexist with the H_1 peak, and these micellar features become more prominent on cooling to lower temperatures (Figure 8). Thus, it appears that there is a coexistence between an isotropic micellar phase and the hexagonal phase and that the micelle-like fraction increases on cooling to lower temperatures.

Thus, the following picture emerges from our data: Addition of PNIPAM to surfactant/water systems results in slightly destabilizing the H_1 phase—the hexagonal phase forms only at higher surfactant concentrations, and the H_1−isotropic transition temperatures decrease by a few degrees. In isotropic micellar surfactant solutions, weak PNIPAM−surfactant interactions result in minor, if any, change in the PNIPAM LCST. However, in the H_1 phase, the PNIPAM LCST is a strong function of surfactant concentration. On cooling, the PNIPAM−surfactant/water system, a surfactant hexagonal mesophase forms. The PNIPAM globules that phase separate from the H_1 phase aggregate at the boundaries of the hexagonal phase domains. The hexagonal phase competes with the PNIPAM for water, and PNIPAM globules are unable to expand to the coil state, until they are cooled to significantly lower temperatures relative to the aqueous PNIPAM transition temperature. At lower temperatures, the PNIPAM chains expand and locally disrupt the H_1 phase organization to form microscopic domains with isotropic micelles in the vicinity of the chains. However, we do not observe any significant decrease in the H_1 phase peaks on cooling, indicating that only a very small fraction of the surfactant in the H_1 phase is disordered to the isotropic micellar state due to the PNIPAM volume transition.

When we compare experiments on 50% $C_{12}E_9$ systems containing 3%, 5%, and 7% PNIPAM, we see that there is little difference in the H_1−isotropic transition temperatures observed in these systems (data not presented). Further, the onset of turbidity on heating also happens at almost the same temperature for all three systems (between 13 and 16 °C). However, there is a systematic increase in room temperature turbidity with increase in PNIPAM content. These results are in accord with our model. With increase in PNIPAM content, there is an increase in the phase-separated PNIPAM globules at room temperature and, therefore, an increase in the sample turbidity. At the same time, the local environment around the phase-separated PNIPAM globules corresponds (in all three cases) to a 50% $C_{12}E_9$ H_1 phase. Thus, the decrease in the onset temperature for turbidity is similar for all three samples.

The competition between hydration of the PNIPAM and swelling of the H_1 phase that we observe might be similar to the microscopic phase separation observed by Pacios et al.,[50] who have investigated a noninteracting polymer [poly(*N,N*-dimethylacrylamide)] in a lamellar AOT/water system.

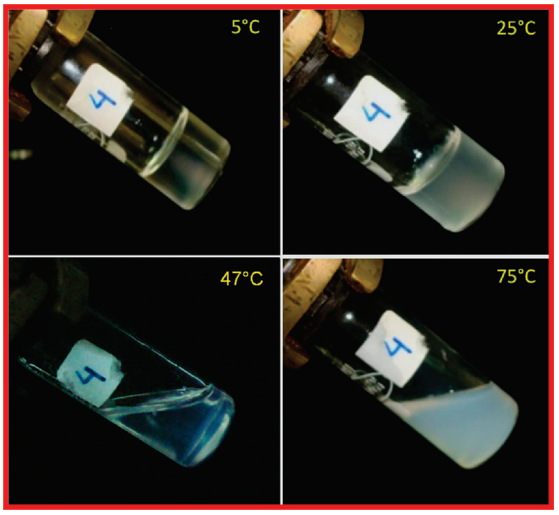

Figure 9. Photographs of 5% PNIPAM copolymer−50% $C_{12}E_9$ system showing the transition from the highly turbid, high-temperature, low-viscosity state (75 °C, bottom right) to the relatively translucent, low-viscosity phase at 47 °C (bottom left), to the turbid gel at room temperature (top right), to the clear gel at 5 °C (top left). The sample vials are tilted to distinguish the low-viscosity materials from the gels.

In their work, water from the lamellar phase hydrates the locally phase-separated polymer coils (driven by the osmotic pressure of the polymer) and results in a deswelled lamellar phase and a polymer-rich isotropic phase. Pacios et al. have also observed that for addition of low molecular weight polymer the polymer simply templates the lamellar phase, while microphase separation happens for the higher molecular weight polymers,[51] and that addition of polymers with a broad molecular weight distribution to the lamellar phase results in segregation of low molecular weight polymers in the lamellar phase and separation of the high molecular weight polymers into the isotropic phase.[52]

Experiments with a PNIPAM Copolymer. To test our proposed mechanism, we now consider a PNIPAM copolymer with a higher transition temperature. Copolymerizing PNIPAM with acrylamide allows us to systematically increase the coil−globule transition temperature by controlling the incorporation of acrylamide. For a PNIPAM copolymer (synthesized with the feed containing 20 wt % of acrylamide), the coil−globule transition temperature in aqueous solution is around 50 °C. When we consider a 5% solution of such a copolymer in a 50% surfactant solution, we observe very interesting behavior (Figure 9). At high temperatures, above 55 °C, the solution is highly turbid since the copolymer is in the collapsed globule state and is aggregated. On cooling to 47 °C (above the surfactant isotropic−H_1 phase transition temperature), the polymer undergoes an expansion to a coil state. The copolymer coils in the isotropic micellar surfactant phase form a translucent solution (Figure 9, bottom left). Copolymerizing the PNIPAM with acrylamide renders it more hydrophilic—therefore, in a solution containing 50% surfactant (viz. with a significantly lower dielectric constant relative to water), it does not form a clear solution but remains translucent. On further cooling, the H_1 phase forms (around 44 °C). The formation of the surfactant H_1 phase results in an increase in turbidity, and we obtain a turbid gel. We interpret this as arising from dehydration of the copolymer coils that collapse again to form globules and aggregate at the H_1 domain boundaries to scatter light. Finally, on equilibrating at even lower temperatures (5 °C), the copolymer globules re-expand and the gel becomes transparent again, in good accord with our proposed mechanism for the behavior of PNIPAM/surfactant mesophase systems.

Conclusions

We describe, for the first time, the influence of the phase of a surfactant matrix on the volume transition of PNIPAM. We select a nonionic surfactant/water system, since PNIPAM−nonionic surfactant interactions are known to be weak. Turbidity measurements indicate that PNIPAM volume transition temperature is not significantly altered in the isotropic micellar surfactant phase, even for surfactant concentrations as high as 42%. However, in the hexagonal mesophase, the PNIPAM volume transition temperature decreases dramatically, as a result of competition between the PNIPAM and the mesophase to associate with water. In the mesophase, the PNIPAM globules phase separate and aggregate at the domain boundaries to form a turbid gel. The PNIPAM chains are able to expand to coils only on cooling to significantly lower temperatures compared with the aqueous coil−globule transition temperature. Thus, the turbid gel becomes clear again at lower temperatures.

Acknowledgment. We acknowledge helpful discussions with Dr. Ashish Lele (NCL), based on which we performed experiments with the PNIPAM copolymer.

Supporting Information Available: Turbidity experiments at different heating rates, hysteresis in turbidity experiments, and NMR data. This material is available free of charge via the Internet at http://pubs.acs.org.

References and Notes

(1) Shibayama, M.; Morimoto, M.; Nomura, S. *Macromolecules* **1994**, *27*, 5060.
(2) Yameen, B.; Ali, M.; Neumann, R.; Ensinger, W.; Knoll, W.; Azzaroni, O. *Small* **2009**, *5*, 1287.
(3) Beverley, R. T.; Carolina de las, H. A.; David, C.; Matthieu, L.; Sivanand, P.; James, R. S.; Dariusz, C. G.; Cameron, A. *J. Controlled Release* **2004**, *97*, 551.
(4) Zha, L.; Zhang, Y.; Yang, W.; Fu, S. *Adv. Mater.* **2002**, *14*, 1090.
(5) Feil, H.; Bae, Y. H.; Feijen, J.; Kim, S. W. *Macromolecules* **1993**, *26*, 2496.
(6) Ringsdorf, H.; Simon, J.; Winnik, F. M. *Macromolecules* **1992**, *25*, 7306.
(7) Ringsdorf, H.; Simon, J.; Winnik, F. M. *Macromolecules* **1992**, *25*, 5353.
(8) Eliassaf, J. *J. Appl. Polym. Sci.* **1978**, *22*, 873.
(9) Freitag, R.; Flaudy, F. G. *Langmuir* **2002**, *18*, 3434.
(10) Kim, Y. H.; Kwon, I. C.; Bae, Y. H.; Kim, S. W. *Macromolecules* **1995**, *28*, 939.
(11) Hofmann, C.; Schönhoff, M. *Colloid Polym. Sci.* **2009**, *287*, 1369–1367.
(12) Meewes, M.; Ricka, J.; De silva, M.; Nyffenegger, R.; Binkert, T. *Macromolecules* **1991**, *24*, 5811.
(13) Schild, H. G.; Tirrell, D. A. *Langmuir* **1990**, *7*, 665.
(14) Ricka, J.; Meewes, M.; Nyffenegger, R.; Binkert, T. *Phys. Rev. Lett.* **1999**, *65*, 657.
(15) Lee, L. T.; Cabane, B. *Macromolecules* **1997**, *30*, 6559.
(16) Wu, X. Y.; Pelton, R. H.; Tam, K. C. *J. Polym. Sci., Part A: Polym. Chem.* **1992**, *31*, 957.
(17) Tam, K. C.; Wu, X. Y.; Pelton, R. H. *J. Polym. Sci., Part A: Polym. Chem.* **1993**, *31*, 963.
(18) Anitha, C. K.; Himadri, B. B.; Ashok, K. M. *Colloids Surf., B* **2008**, *70*, 60.
(19) Loh, W.; Teixeira, L. A.; Lee, L. T. *J. Phys. Chem. B* **2004**, *108*, 3196.
(20) Winnik, F. M.; Ringsdorf, H.; Venzmer, J. *Langmuir* **1990**, *7*, 912.
(21) Kokufuta, E.; Zang, Y. Q.; Tanaka, T.; Mamada, A. *Macromolecules* **1992**, *26*, 1053.
(22) Wu, C.; Zhou, S. *J. Polym. Sci., Part B: Polym. Phys.* **1996**, *34*, 1597.
(23) (a) Wong, J. E.; Richering, W. *Prog. Colloid Polym. Sci.* **2006**, *133*, 45. (b) Wong, J. E.; Muller, C. B.; Laschewsky, A.; Richtering, W.

J. Phys. Chem. B **2007**, *111*, 8527. (c) Wong, J. E.; Richtering, W. *Curr. Opin. Colloid Interface Sci.* **2008**, *13*, 403. (d) Wong, J. E.; Diez-Pascual, A. M.; Richtering, W. *Macromolecules* **2009**, *42*, 1229.
(24) Jean, B.; Lee, L. T. *J. Phys. Chem. B* **2005**, *109*, 5162.
(25) Jean, B.; Lee, L. T.; Cabane, B.; Bergeron, V. *Langmuir* **2009**, *25*, 3966.
(26) Ding, Y.; Zhang, G. *J. Phys. Chem. C* **2007**, *111*, 5309–5312.
(27) Choi, J. H.; Lee, H. Y.; Kim, J. C.; Kim, Y. C. *J. Ind. Eng. Chem.* **2007**, *13*, 380.
(28) Kumaraswamy, G.; Wadekar, M. N.; Vikrant, V. A.; Pasricha, R. *Polymer* **2005**, *46*, 7961.
(29) Wadekar, M. N.; Pasricha, R.; Gaikwad, A. B.; Kumaraswamy, G. *Chem. Mater.* **2005**, *17*, 2460.
(30) Sharma, K. P.; Kumaraswamy, G.; Isabelle, L.; Mondain-Monval, O. *J. Phys. Chem. B* **2009**, *113*, 3423.
(31) Durand, A.; Hourdet, D. *Polymer* **1999**, *40*, 4941.
(32) Shen, Z.; Terao, K.; Maki, Y.; Dobashi, T.; Ma, G.; Yamamoto, T. *Colloid Polym. Sci.* **2006**, *284*, 1001.
(33) Hoffman, A. S.; Stayton, P. S.; Bulmus, V.; Chen, G.; Chen, J.; Cheung, C.; Chilkoti, C.; Ding, Z.; Dong, L.; Fong, R.; Lackey, C. A.; Long, C. J.; Miura, M.; Morris, J. E.; Murthy, N.; Nabeshima, Y.; Park, T. G.; Press, O. W.; Shimoboji, T.; Shoemaker, S.; Yang, H. J.; Monji, N.; Nowinski, R. C.; Cole, C. A.; Priest, J. H.; Harris, J. M.; Nakamae, K.; Nishino, T.; Miyata, T. *J. Biomed. Mater. Res., Part A* **2000**, *52*, 577.
(34) Vold, R. L.; Waugh, J. S.; Klein, M. P.; Phelps, D. E. *J. Chem. Phys.* **1968**, *48*, 3831.
(35) Freeman, R.; Hill, H. D. W. *J. Chem. Phys.* **1969**, *51*, 3140.
(36) Bax, A.; Davis, D. G. *J. Magn. Reson.* **1985**, *63*, 207.
(37) Spevacek, J. *Curr. Opin. Colloid Polym. Sci.* **2009**, *14*, 184.
(38) Yoshioka, H.; Mori, Y.; Cushman, J. A. *Polym. Adv. Technol.* **1994**, *5*, 122.
(39) Griffiths, P. C.; Stilbs, P.; Chowdhry, B. Z.; Snowden, M. J. *Colloid Polym. Sci.* **1995**, *273*, 405.
(40) Tanaka, N.; Matsukawa, S.; Kurosu, H.; Ando, I. *Polymer* **1998**, *39*, 4703.
(41) Starovoyatova, L.; Spevácek, J.; Hanykova, L.; Ilavský, M. *Macromol. Symp.* **2003**, *203*, 239.
(42) Starovoytova, L.; Spevacek, J. *Polymer* **2006**, *47*, 7329.
(43) Ray, S. S.; Rajamohanan, P. R.; Badiger, M. V.; Devotta, I.; Ganapathy, S.; Mashelkar, R. A. *Chem. Eng. Sci.* **1998**, *53*, 867.
(44) Badiger, M. V.; Rajamohanan, P. R.; Kulkarni, M. G.; Ganapathy, S.; Mashelkar, R. A. *Macromolecules* **1991**, *24*, 106.
(45) Zeng, F.; Tong, Z.; Feng, H. *Polymer* **1997**, *38*, 5539.
(46) Spevácek, J.; Geschke, D.; Ilavský, M. *Polymer* **2001**, *42*, 463.
(47) Rajamohanan, P. R.; Badiger, M. V.; Ganapathy, S.; Mashelkar, R. A. *Macromolecules* **1991**, *24*, 1423.
(48) Burba, C. M.; Carter, S. M.; Meyer, K. J.; Rice, C. V. *J. Phys. Chem. B* **2008**, *112*, 10399.
(49) Neuhaus, D.; Williamson, M. *The Nuclear Overhauser Effect in Structural and Conformational Analysis*; VCH: New York, 1989.
(50) Pacios, I. E.; Renamayor, C. S.; Horta, A.; Lindman, B.; Thuresson, K. *J. Phys. Chem. B* **2002**, *106*, 5035.
(51) Pacios, I. E.; Renamayor, C. S.; Horta, A.; Thuresson, K.; Lindman, B. *Macromolecules* **2005**, *38*, 1949.
(52) Pacios, I. E.; Renamayor, C. S.; Horta, A.; Lindman, B.; Thuresson, K. *J. Phys. Chem. B* **2005**, *109*, 23896.